

Numerical Investigation on The Combustion and Flow Characteristics of Ammonia in Nozzle

Nianduo Song, Fei Wang, Xinlin Xia*

Key Laboratory of Aerospace Thermophysics of MIIT, School of Energy Science and Engineering, Harbin Institute of Technology
No. 92, West Dazhi Street, Harbin, Heilongjiang 150001, China
xiaxl@hit.edu.cn

Abstract - Ammonia energy has good prospects for development. In order to utilize ammonia more effectively, the combustion characteristics of ammonia in the nozzle are investigated in this paper. The velocity, pressure, and temperature distributions in the nozzle are analyzed by comparing four different mass flow ratios of air and ammonia mixture. Case I has the highest outlet velocity of 1780 m/s and the maximum outlet average velocity of 1690 m/s, and Case IV has the largest average outlet pressure of 2826 Pa. The magnitude of the thrust produced by the nozzle is related to the mass flow rate at the nozzle outlet and the intensity of the chemical reaction inside the nozzle. The maximum thrust is 121 N, obtained in Case IV.

Keywords: Ammonia combustion; High-temperature; Carbon-free fuel; Nozzle;

1. Introduction

Ammonia has a high energy density and can be obtained from renewable energy sources such as fossil fuels and biomass. [1] Ammonia, as a mature industrial product, has complete production and transportation conditions. As a carbon-free fuel, it has attracted increasing attention [2]. Therefore, studying the combustion characteristics of ammonia is of great significance.

In recent years, many people have conducted extensive research on the combustion of ammonia gas. Hayakawa [3] studied the unstretched laminar combustion velocity and Markstein length of ammonia/air-premixed flames at various pressures up to 0.5 MPa. Their findings indicate that the maximum value of unstretched laminar combustion velocity is lower than that of hydrocarbon flames, less than 7cm/s. Lhuillier [4] et al. Investigated the combustion characteristics of ammonia through laminar and turbulent diffusion flame experiments using an electric spark ignition engine. The experimental results indicate that doping hydrogen into ammonia increases the heat release rate of the flame, while doping methane reduces the heat release rate of the flame. Lamoureux [5] conducted temperature tests on ammonia methane mixed fuel with methane as the main fuel using a water-cooled brass burner with an inner diameter of 68 mm. At a total inlet flow rate of 5.5 L/min, the highest flame temperature under preset conditions reached 1770 K. Mendiara [6] studied the effect of increased carbon dioxide content on the generation of other combustion products during the ammonia methane oxidation process. Their research found that when the carbon dioxide content in the combustion products increased, the OH/H ratio increased, thereby promoting the generation of nitric oxide.

This article analyzes the combustion characteristics of ammonia. It mainly considers the reaction between ammonia and oxygen in the air to produce nitrogen dioxide and water, as shown in Eq. (1). By setting the nozzle structure, compare the reaction process of air and ammonia with different mass flow rates. Explore the variation patterns of parameters such as outlet velocity and density of the nozzle.



2. Problem description

2.1. Equations

The flow, heat transfer, and component transport govern equations for gas mixtures can be written in a general form with the general variable ϕ , which reads as:

$$\frac{\partial(\rho\phi)}{\partial t} + \nabla \cdot (\rho\vec{V}\phi) = \nabla \cdot (\Gamma_\phi \nabla \phi) + S_\phi \quad (2)$$

The terms in Eq. (2) are transient term, convective term, diffusion term, and source term in that order. Table 1 shows the specific form of the generic variable in the general equation Eq. (2).

Table 1: Specific forms of symbols in general equations.

	ϕ	Γ_ϕ	S_ϕ
Continuity Equation	1	0	0
Momentum Equation	\vec{V}	μ	$-\nabla p + \vec{S}_M$
Energy Equation	T	λ/c	S_T/c
Species Equation	Y_i	$\rho_i D_i$	S_i

2.2. turbulence model and chemical dynamics

The original $k-\omega$ model performs better near the wall, whereas the standard $k-\varepsilon$ model needs to cooperate with a wall function in order to compute high Reynolds number flows, the $k-\omega$ SST model developed on this basis combines the advantages of both and can accurately calculate the heat transfer near the wall. Therefore, the $k-\omega$ SST model is adopted to calculate the turbulent flow in this work.

In high Reynolds number flows, chemical reaction kinetics are controlled by turbulent eddy strength rather than the traditional finite rate model. The net production rates of components are given by the smaller of Eq. (3).

$$R_{i,r} = v'_{i,r} M_{w,i} A B \rho \frac{\varepsilon}{k} \frac{\sum_j^N Y_j}{\sum_j^N v'_{j,r} M_{w,j}}, \quad R_{i,r} = v'_{i,r} M_{w,i} A \rho \frac{\varepsilon}{k} \min\left(\frac{Y_j}{v'_{j,r} M_{w,j}}\right) \quad (3)$$

where Y is the mass fraction, A and B are the empirical constants, with values of 4.0 and 0.5 respectively, and the subscripts j and i refer to the species index.

2.3. Boundary conditions and geometric modeling

The computational model and boundary conditions are shown in Fig. 1, where air is injected into Inlet 1 and ammonia into Inlet 2. The walls were assumed to be adiabatic with an emissivity of 0.8 and the outlet is set to a constant pressure. The specific boundary conditions are listed in Table 2.

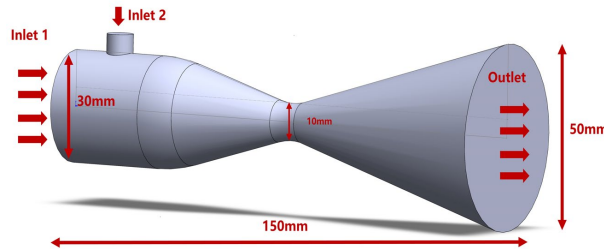


Fig. 1: Geometric model of nozzle

Table 2: Properties of materials

Case	Inlet 1 Temperature (K)	Inlet 2 Temperature (K)	Inlet 1 Mass Flow (g/s)	Inlet 2 Mass Flow (g/s)	Total Mass Flow (g/s)
Case I	873	973	15	5	20
Case II	873	973	20	5	25
Case II	873	973	25	5	30
Case IV	873	973	30	5	35

3. Results and discussion

3.1. Calculation of nozzle operating conditions

The temperature, pressure, and velocity distributions inside the nozzle at different mass flow ratios are shown in Figs. 2, 3, and 4, respectively. Case I has the highest temperature of 1622 K. For the velocity at the outlet, Case I gives the highest value of 1780 m/s and the maximum and average value of 1690 m/s. In addition, the maximum average outlet pressure of 2826 Pa is obtained in Case IV.

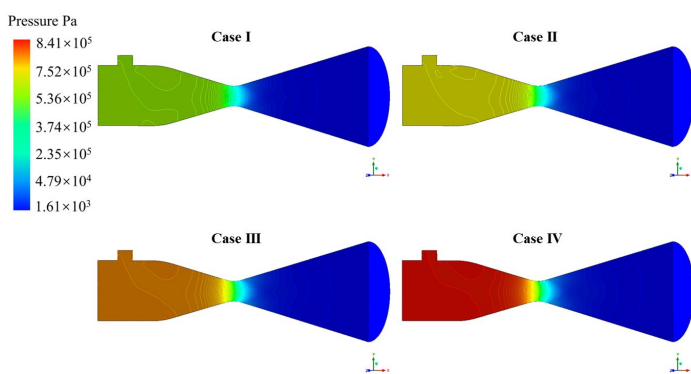


Fig. 2: Pressure distribution map inside the nozzle

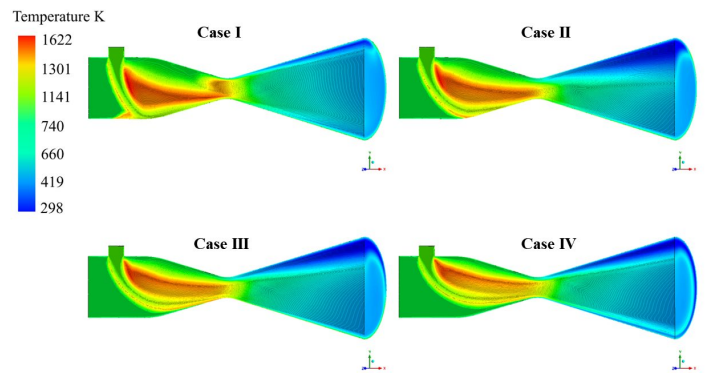


Fig. 3: Temperature distribution map inside the nozzle

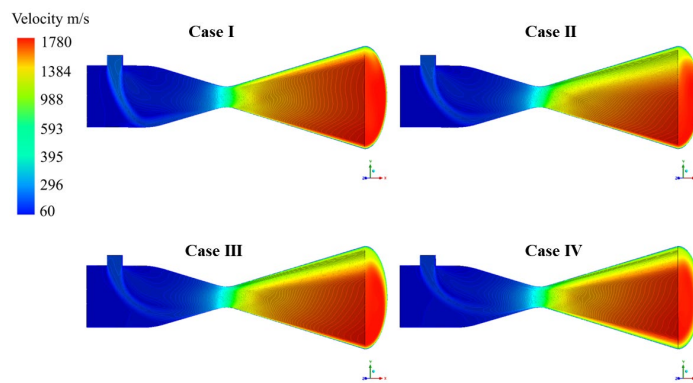


Fig. 4: Velocity distribution map inside the nozzle

3.2. Thrust calculation

The thrust of the nozzle is influenced by the mass flow rate and the ambient pressure at the outlet, which can be calculated according to the following:

$$\vec{F} = \dot{m}\vec{V}_e + A_e(p_e - p_a)\vec{n} \quad (4)$$

where \dot{m} is the mass flow rate, \vec{v}_e is the outlet velocity, A_e is the area at the outlet, p_e is the outlet pressure, p_a is the ambient pressure, and \vec{n} is the unit normal vector at the outlet.

We analyzed and calculated the mass flow rate and pressure at the outlet of air-ammonia mixed combustion at ratios to obtain the magnitude of thrust generated by the air-ammonia fuel under the corresponding working conditions. specific values are shown in Table 3. From the data in the table, it can be seen that Case IV has the largest thrust.

Table 3: Nozzle outlet condition

Case	Average outlet velocity (m/s)	Average outlet density (kg/m ³)	Average outlet pressure (Pa)	Thrust (N)
Case I	1690	0.0122	1713	71.7
Case II	1651	0.0159	2058	89.1
Case III	1619	0.0197	2391	106.3
Case IV	1565	0.0240	2862	121.0

4. Conclusion

This work explores the combustion characteristics of ammonia by injecting air and ammonia with different mass flows into a nozzle for combustion, and draws the following conclusions:

1. The maximum temperature for combustion of air-ammonia mixtures and the maximum average velocity at the outlet is obtained in Case I of value 1622 K and 1690 m/s.
2. Case IV has the maximum mean pressure at the outlet with values of 2826 Pa.
3. The thrust generated by the nozzle is mainly related to the mass flow rate of the nozzle and the intensity of the chemical reaction. Case IV generated the maximum thrust of 121 N.

References

- [1] H. Kobayashi, A. Hayakawa. "Science and technology of ammonia combustion," *P. Combust Inst.*, vol. 37, no. 1, pp. 109-133, 2019.
- [2] W. Wang, J. M. Herreros. "Ammonia as hydrogen carrier for transportation; investigation of the ammonia exhaust gas fuel reforming," *P. Combust Inst., Int J. Hydrogen Energ.*, vol. 38, no. 23, pp. 9907-9917, 2013.
- [3] A. Hayakawa, T. Goto, R. Mimoto. "Laminar burning velocity and markstein length of ammonia/air premixed flames at various pressures," *Fuel*, vol. 159, no. 1, pp. 98-106, 2015.
- [4] C. Lhuillier, P. Brequigny, F. Contino. "Experimental investigation on ammonia combustion behavior in a spark-ignition engine by means of laminar and turbulent expanding flames," *P. Combust Inst.*, vol. 58, no. 8, pp. 1-10, 2020.
- [5] N. Lamoureux, P. Dsegroux, L. Gasnot. "Measurements and Modelling of Nitrogen Species in CH₄/O₂/N₂ Flames Doped with NO, NH₃, or NH₃+NO," *Combust Flame.*, vol. 176, pp. 48-59, 2017.
- [6] T. Mendiara, P. Glarborg. "Ammonia Chemistry in Oxy-Fuel Combustion of Methane," *Combust Flame.*, vol. 156, no. 10, pp. 1937-1949, 2009.